nature geoscience

LETTERS

PUBLISHED ONLINE: 5 SEPTEMBER 2013 | DOI: 10.1038/NGEO1936

A weak El Niño/Southern Oscillation with delayed seasonal growth around 4,300 years ago

H. V. McGregor[1]*, M. J. Fischer[2], M. K. Gagan[3], D. Fink[2], S. J. Phipps[4], H. Wong[2] and C. D. Woodroffe[1]

Earth's interannual climate variability is dominated by El Niño/Southern Oscillation (ENSO). Palaeoclimate records indicate a lower ENSO variance during the middle Holocene compared with today[1–6]; however, model simulations have not reproduced the full magnitude of the changes[7–10], and whether external forcing drives large intrinsic ENSO variability[11] is therefore a matter of considerable debate. Here we present a 175-year-long, monthly resolved oxygen isotope record, obtained from a *Porites* coral microatoll located on Kiritimati (Christmas) Island, in the NINO3.4 region of the central equatorial Pacific. Our quantitative record of ENSO variability about 4,300 years ago shows that ENSO variance was persistently reduced by 79%, compared with today, and it exhibits a dominant annual cycle. Season-specific analysis shows that El Niño events were damped during their September–November growth phase, and delayed relative to the climatological year. We suggest that the higher boreal summer insolation at the time strengthened the tropical Pacific zonal winds as well as the gradients in sea surface temperature, and thereby led to an enhanced annual cycle and suppressed ENSO. As the weak ENSO is subject to interdecadal amplitude modulation, we conclude that amplitude modulation is likely to remain robust under altered climates. Our findings show that ENSO is capable of responding to external forcing.

ENSO is a tropical ocean–atmospheric phenomenon that oscillates irregularly every 2–8 years, and disrupts rainfall patterns around the globe[12]. The mean state of the equatorial Pacific Ocean involves easterly trade winds that push warm water westward. During an El Niño event, these winds slacken allowing warm water to flow eastward. This reduces the east–west equatorial ocean temperature gradient, giving rise to positive sea surface temperature (SST) anomalies in the central and eastern equatorial Pacific. Atmospheric convection follows the warmest water eastward, causing major changes in rainfall. Short-term forecasts of El Niño events are routine, but understanding the behaviour of ENSO under different climate states is still problematic[13–15]. Importantly, alternative ENSO behaviours may dominate under global warming[16], posing a serious challenge for successful adaptation to climate change.

Reconstruction of past ENSO dynamics from coral, tree ring, and sediment-derived climatic archives offers the prospect of understanding its different modes and responses to altered boundary conditions[1–6,11,17–19]. These reconstructions show an overall increase in ENSO frequency and magnitude that began about 6,500 years before the present[1–6] (6.5 kyr BP). A number of studies have argued that changes in Earth's orbital geometry influenced ENSO through the Holocene epoch[7–9,20]; however, recent work challenges this view[11]. Three limitations prevent detection of past changes in records of ENSO variability and characteristics: most records are limited to annual or coarser resolution[2,4,5] that obscure the influence of seasonality[20]; seasonally resolved records[1,3] are generally too short to demonstrate that changes are not due to stochastic (random) internal variability[11,21]; and most records are located beyond ENSO core regions and may not directly reflect ENSO changes, but rather changes in the teleconnection to ENSO. Quantitative reconstruction of palaeo-ENSO variance requires a natural archive from the core ENSO region that is seasonally resolved and sufficiently long to capture both seasonal and interdecadal influences[21].

In this study, we present a continuous 175-year-long, monthly resolved $\delta^{18}O$ record for a fossil *Porites* coral microatoll from Kiritimati (Christmas) Island (1° 44.21′ N, 157° 12.52′ E) dating to ~4.3 kyr BP (coral XM35, hereafter the ~4.3 kyr BP coral; Methods and Supplementary Methods). Kiritimati is an optimal site[22] in the NINO3.4 region, which serves to circumvent many of the uncertainties associated with palaeo-ENSO records.

The ~4.3 kyr BP coral $\delta^{18}O$ record shows distinct differences in ENSO behaviour compared with the present day (Fig. 1a,c). We find a 79% reduction in variance for the 2–8-year frequency band ($\sigma^2 = 0.0035‰^2$) compared with a stacked modern coral $\delta^{18}O$ record from Kiritimati ($\sigma^2 = 0.0169‰^2$; Supplementary Table S3). The power spectrum of the interannual time series for the ~4.3 kyr BP $\delta^{18}O$ record shows peak variance between 6 and 8 years, indicating that ENSO events were less frequent than at present (Fig. 1d). Cluster analysis shows that El Niño and La Niña events occur as only weak–moderate $\delta^{18}O$ anomalies at ~4.3 kyr BP (Supplementary Methods), with a distinct absence of the moderate–strong $\delta^{18}O$ anomalies that characterize the present day (Fig. 2). Further statistical testing and comparisons with climate model simulations suggest that the reduction in ENSO variance is highly unlikely an artefact of sampling unusual ENSO variability within a short time window, and that the ENSO variance lies outside that expected from unforced internal variability within the ENSO system (Supplementary Discussion). Importantly, the ~4.3 kyr BP coral exhibits reduced variance compared with both the Holocene and the instrumental baseline of ENSO variance[11] (Supplementary Fig. S8).

Previous investigations of past ENSO have focused on changes in variability alone[1–4,6,11]. Our results support the idea that ENSO variability was reduced during the middle Holocene[1–6] (6.5–4 kyr BP). The persistent reduction in variance at ~4.3 kyr BP is

[1]School of Earth and Environmental Sciences, University of Wollongong, New South Wales 2522, Australia, [2]Institute for Environmental Research, Australian Nuclear Science and Technology Organisation, Locked Bag 2001, Kirrawee DC, New South Wales 2232, Australia, [3]Research School of Earth Sciences, The Australian National University, Canberra, Australian Capital Territory 0200, Australia, [4]Climate Change Research Centre and ARC Centre of Excellence for Climate System Science, University of New South Wales, Sydney, New South Wales 2052, Australia. *e-mail: mcgregor@uni-bremen.de

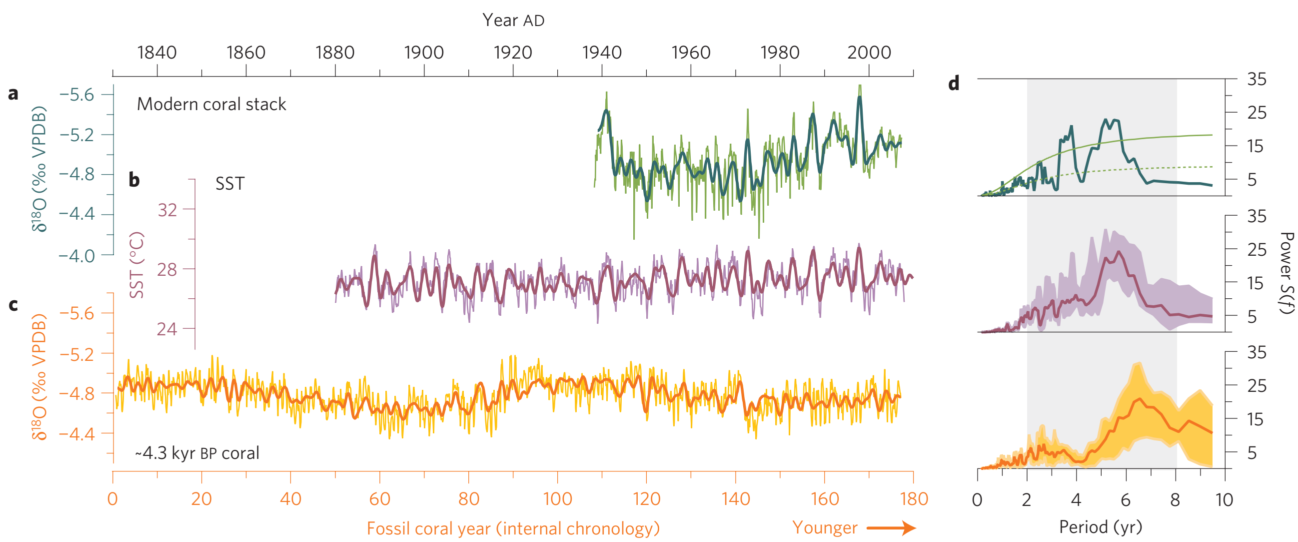

Figure 1 | Comparison of Kiritimati coral δ^{18}O and instrumental SST. a, Stacked modern coral δ^{18}O (refs 3,22,24; Supplementary Fig. S4). **b**, SST (ref. 30) for 158° W, 2° N, scaled to coral δ^{18}O (−0.15‰ per degree Celsius[24]). **c**, ∼4.3 kyr BP coral δ^{18}O. Bold lines in **a**–**c** show 2–8-year Butterworth band-pass filtering plus the trend (Supplementary Methods). **d**, Interannual power spectra for modern coral δ^{18}O (dark green), with mean red noise spectrum (dashed line) and 95% confidence interval (solid line). Interannual power spectra for 69-year moving windows (1-month step) and 2.5–97.5% quantiles (shading) for Kiritimati SST (purple) and ∼4.3 kyr BP coral δ^{18}O (orange). Grey shading indicates 2–8-year ENSO periodicities.

similar in magnitude to the 85% reduction in ENSO variance seen in ∼6.5–4 kyr BP tropical Pacific corals[1,11], but the reduction is significantly larger than that simulated by ENSO modelling studies[7–10].

A critical aspect of the ∼4.3 kyr BP δ^{18}O record is that the 175 years of coral growth contain sufficient El Niño and La Niña events to formulate an accurate picture of the seasonal evolution of a typical event ∼4,300 years ago. Understanding the seasonal-scale dynamics of ENSO is important because it points to the processes that may link climate forcing and the development of El Niño events. Today, El Niño events are phase-locked to the annual cycle, whereby their growth, peak and decay follow a characteristic pattern relative to the climatological year. El Niño anomalies in equatorial Pacific SSTs typically emerge in boreal summer (June–August), increase during boreal autumn (September–November) and peak during boreal winter (December–February). Importantly, this pattern is evident in Kiritimati SSTs and is replicated in modern coral δ^{18}O records (Fig. 2d,e and Supplementary Methods).

The seasonal characteristics of El Niño anomalies at ∼4.3 kyr BP are suppressed and shifted relative to modern El Niño events. Cluster analysis of the ∼4.3 kyr BP δ^{18}O record shows that El Niño events are damped during the boreal autumn growth phase (September–November), peak at the end of boreal winter (February) and then slowly decay (Fig. 2f). The cluster analysis also shows that La Niña anomalies are reduced and delayed by two–three months compared with the present (Fig. 2).

A partial modern analogue for ENSO behaviour at ∼4.3 kyr BP may be the ENSO quiescent period of the 1920–1950s. This well-documented interval of reduced ENSO variability is thought to be related to an enhanced annual cycle at that time, particularly in the east Pacific[17,23]. The amplitude of the average annual cycle of coral δ^{18}O is 0.22 ± 0.02‰ 2σ at ∼4.3 kyr BP, which is larger than the 0.17 ± 0.06‰ 2σ seasonality in the stacked 1978–2007 modern coral δ^{18}O record[3,24] (Fig. 3a and Supplementary Methods). The 1978–2007 δ^{18}O stack excludes the potential impact of 1–2-month δ^{18}O spawning spikes[22] (Supplementary Fig. S4). Strong El Niño years were also excluded from the average annual cycle estimate for the fossil and modern corals because ^{18}O-depleted rainfall lowers the δ^{18}O of sea water during El Niño years ($\delta^{18}O_{sw}$; Supplementary Fig. S9). Furthermore, coral Sr/Ca thermometry demonstrates that SST is the driver of modern and fossil coral δ^{18}O at Kiritimati Island during non-El Niño years, and the influence of any changes in $\delta^{18}O_{sw}$ on the annual cycle of coral δ^{18}O is negligible[22] (Supplementary Discussion). The annual cycle amplitude difference between the modern and ∼4.3 kyr BP corals is statistically significant, being greater than a one-sided 95% confidence interval for the null hypothesis that there is no difference in the annual cycle amplitude of two time series (Supplementary Discussion).

The relationship between the enhanced annual cycle and reduced interannual variance in the ∼4.3 kyr BP coral record is further highlighted by the ratio of the 2–8-year band ENSO variance to the annual cycle variance. This ratio is only 1.0 for the ∼4.3 kyr BP coral δ^{18}O whereas it is 5.5 for the modern coral δ^{18}O stack (Supplementary Fig. S6 and Table S3). The dominance of the annual cycle over interannual variability in the ∼4.3 kyr BP coral is supported by the Kiritimati fossil coral Sr/Ca–SST results (Supplementary Fig. S6 and Table S3).

Modelling studies suggest that increased insolation seasonality, brought about by Earth's precessional cycle, drives much of the mid-Holocene ENSO reduction[7–9,20]. The altered insolation forcing may act directly on the tropical Pacific, changing the east–west SST gradient during boreal summer and autumn, which in turn enhances the easterly trade winds and suppresses El Niño development[7]. However, global climate models also suggest that the effects of insolation forcing on regions beyond the tropical Pacific are influential[8,9]. For example, increased boreal summer warming over northern mid-latitudes strengthens the Walker circulation and equatorial Pacific easterly wind anomalies in boreal summer and autumn, which would tend to subdue the development of El Niño events[8,9]. Although these processes may be driving some of the mid-Holocene ENSO reduction, they do not fully explain the combination of changes in the annual cycle and ENSO evolution observed at ∼4.3 kyr BP.

The reduced ENSO at ∼4.3 kyr BP could be due to mid-Holocene changes in the annual cycle processes in the eastern and central equatorial Pacific. Today, the annual cycle in this region is inextricably linked to the seasonal evolution of the north–south (meridional) SST gradient across the eastern tropical Pacific[25] (Fig. 3b). Warming north of the Equator in boreal spring and summer drives cross-equatorial winds that converge at the intertropical convergence zone, and over warm waters, and induce

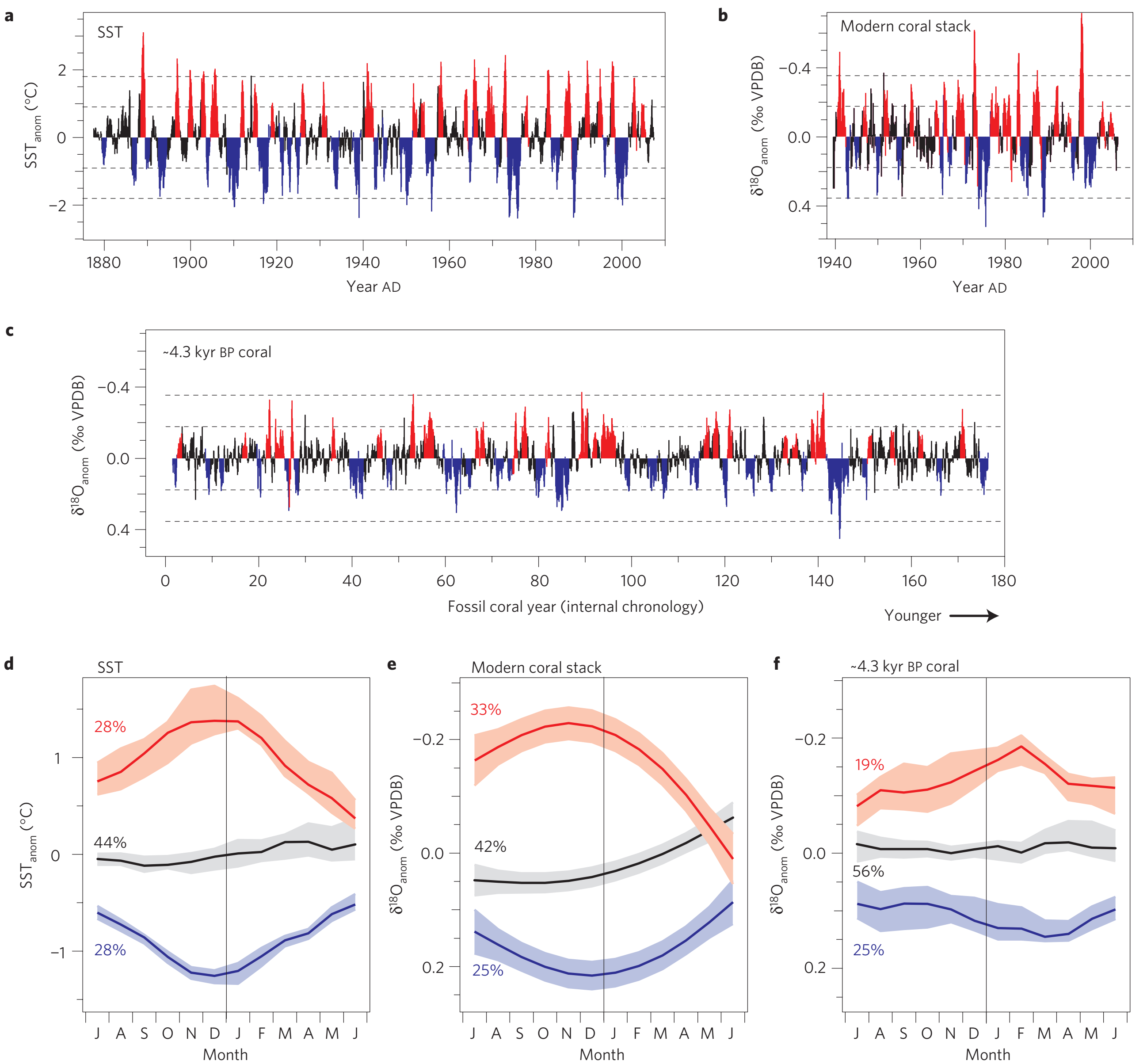

Figure 2 | The interannual and seasonal evolution of ENSO. a, Kiritimati SST (ref. 30) for 1877–2007. **b**, Stacked modern coral δ^{18}O. **c**, ∼4.3 kyr BP coral δ^{18}O. Dashed lines show thresholds for weak ($<1\sigma$), moderate (1σ–2σ) and strong ($>2\sigma$) El Niño (red) and La Niña (blue) events. In **c**, dashed lines are from **b**. **d**–**f**, Composite El Niño (red), La Niña (blue) and neutral (black) years identified by cluster analysis (Supplementary Methods). 95% confidence interval in **e** is shaded. **d**,**f** are calculated on moving 69-year windows (1-year step) with 2.5–97.5% quantiles plotted (shading). Percentages are the frequency of years in each cluster.

upwelling of cooler water in the equatorial region (Fig. 3b). In the following months the cooling strengthens the east–west (zonal) SST gradient, driving the trade winds along the Equator, which reinforces upwelling in the eastern equatorial Pacific (the Bjerknes feedback). Through boreal autumn and winter SSTs north of the Equator decrease, so the meridional SST gradient and eastern equatorial Pacific upwelling also decrease. The annual cycle of SST and modern coral δ^{18}O at Kiritimati Island is a westward extension of the annual cycle in the eastern equatorial Pacific, delayed by several months and reduced in amplitude[24].

The enhanced annual cycle in the ∼4.3 kyr BP coral record could reflect insolation forcing of the annual cycle process described above. At ∼4.3 kyr BP, insolation in the tropics and northern mid-latitudes was higher in boreal summer and early autumn (Supplementary Fig. S11), resulting in increased northern tropical heating and a strengthened and more northerly intertropical convergence zone[26]. This would strengthen the cross-equatorial winds during those months and enhance eastern equatorial Pacific upwelling. As a consequence, the zonal SST gradient and trade winds strengthen, and the annual cycle in the eastern-central equatorial Pacific strengthens too. The outcome would be to suppress initiation of El Niño events in the boreal autumn and early winter. In addition, reduced insolation in boreal spring may cause less direct radiative heating, thus extending the cool season. Overall, this picture is consistent with the enhanced annual cycle and reduced ENSO in the ∼4.3 kyr BP coral record. It is also consistent with proxy evidence of reduced eastern equatorial Pacific SSTs and enhanced upwelling during the middle Holocene[6,27], and with idealized modelling experiments on the effects of orbital forcing on the annual cycle and ENSO (ref. 28).

A confounding issue in ENSO predictability today is understanding interdecadal modulation of ENSO amplitude[13,15,19,29]. The

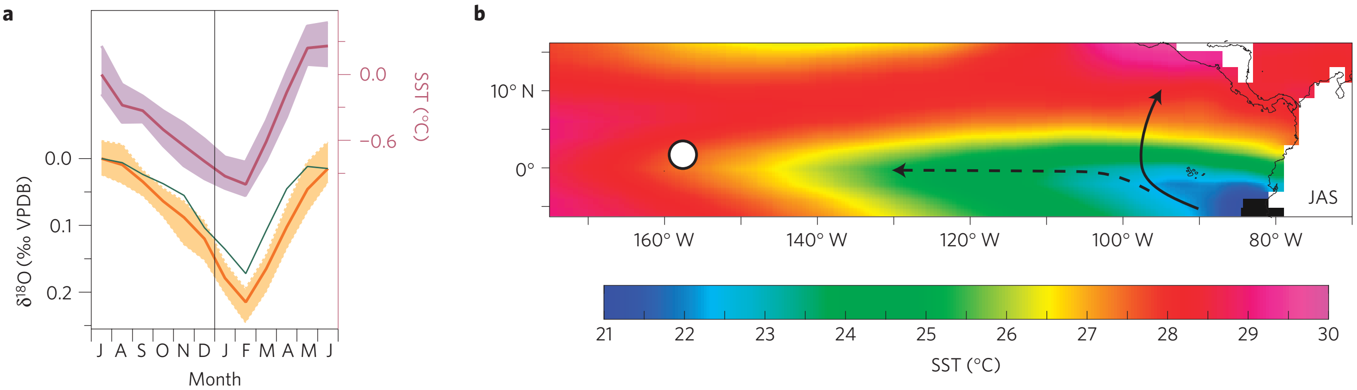

Figure 3 | Annual cycle of the Kiritimati SST, modern coral $\delta^{18}O$ and ~4.3 kyr BP coral $\delta^{18}O$ records. a, Average annual cycle extracted for WM_modern coral $\delta^{18}O$ for 1978–2007 (green; Supplementary Fig. S4). Kiritimati SST (ref. 30; purple) and ~4.3 kyr BP $\delta^{18}O$ (orange) median annual cycle calculated for moving 29-year windows (1-month step) and 2.5–97.5% quantiles (shading; Supplementary Methods). Zero is arbitrarily set to July. **b**, Map of average July–September SST (ref. 30) for 1978–2007. The solid arrow indicates the direction of cross-equatorial winds. The dashed arrow indicates easterly trade winds and the westward extension of cool equatorial SSTs, which reach Kiritimati (white circle) in January–March.

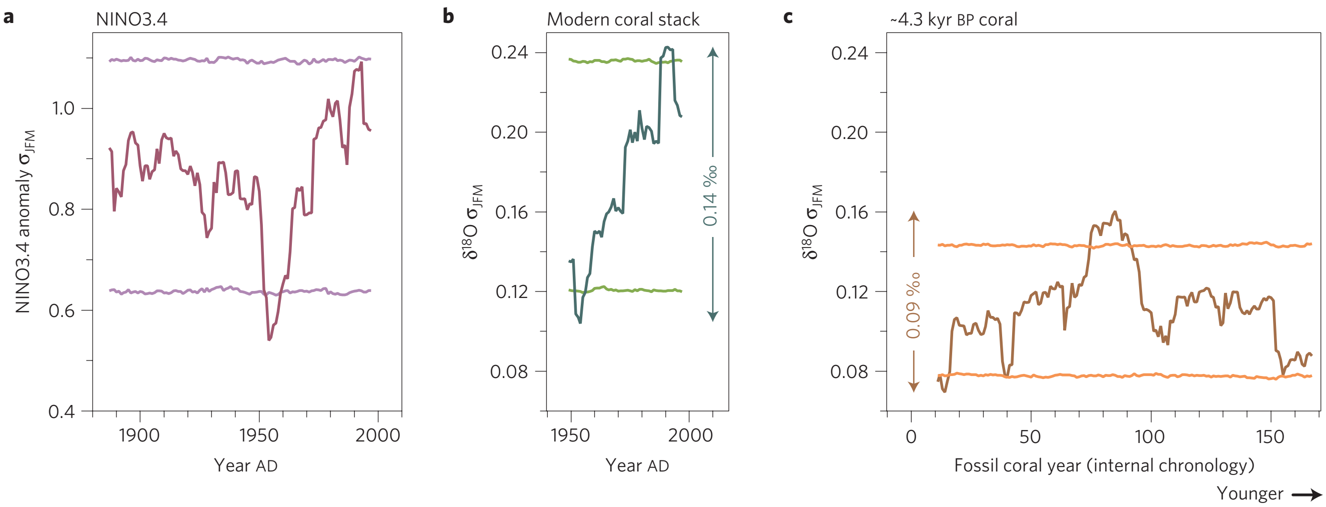

Figure 4 | Interdecadal modulation of ENSO amplitude. a–c, 21-year running standard deviation (σ_{JFM}) of boreal winters (January–March) for NINO3.4 anomaly, stacked modern coral $\delta^{18}O$ and ~4.3 kyr BP coral $\delta^{18}O$ records. Significant interdecadal modulation of ENSO amplitude is indicated by standard deviations exceeding the 95% confidence intervals (near-horizontal lines). These excursions are unlikely to result from variation due to sampling a stationary process over a 21-year time window (Supplementary Methods). Green and brown arrows mark the maximum σ_{JFM} range for modern coral and ~4.3 kyr BP coral $\delta^{18}O$ records, respectively.

175-year length of the ~4.3 kyr BP coral $\delta^{18}O$ record is sufficiently long to show that despite a substantial average reduction, ENSO amplitude is still subject to significant interdecadal modulation, and the absolute modulation at the interdecadal scale can be similar to modern (for example, ~4.3 kyr BP coral years 75–90; Fig. 4). Interdecadal modulation seems to be a feature of the climate system over the past millennium, and has been linked to changes in the mean state of the Pacific climate and global temperature[19,29]. Decadal-scale modulation of ENSO amplitude may also indicate that low-frequency internal variability contributes to the amplitude of ENSO variability. The ~4.3 kyr BP coral record confirms that modulation of ENSO amplitude is a robust feature of the system, and highlights that long records are needed to identify such changes.

Our observations of a broadly weaker ENSO, reduced El Niño growth in boreal autumn, and a delay in the maturation of events document an ENSO response to mid-Holocene insolation forcing through seasonal-scale climate dynamics in the eastern equatorial Pacific. In addition, the interdecadal modulation of ENSO at ~4.3 kyr BP suggests that decadal ENSO variability is likely to persist under the influence of future changes in the mean climate state[13].

Importantly, the altered palaeo-ENSO variance, periodicity and seasonality provide a clear test for climate models to capture the response of ENSO to external forcings. Given the apparent influence of external forcing on the ~4.3 kyr BP coral and the changes in ENSO behaviour through the late twentieth century[16], further understanding of the temporal and spatial evolution of ENSO is essential to improve climate forecasting in a warmer world.

Methods

Living and fossil *Porites* sp. microatolls were collected from Kiritimati Island (1° 50′N, 157° 25′E; Supplementary Fig. S1). Microatolls are large, disc-shaped coral colonies limited in their upward growth by the lowest tides. Their growth is restricted to the uppermost surface waters, which makes them ideal for reconstructing ENSO-related, depth-dependent variables, such as SST and sea surface salinity. The skeletal $\delta^{18}O$ of microatolls living around Kiritimati faithfully registers the warmer SSTs and increased precipitation during El Niño events[3,24] (Fig. 1a and Supplementary Methods). The remarkable 5-m-diameter fossil microatoll, XM35, grew on what was a flourishing mid-Holocene reef. The well-preserved coral (Supplementary Methods and Supplementary Fig. S2 and Table S1) grew continuously for 175 years between ~4.2 and ~4.4 kyr BP, as indicated by an average U-series age of 4,243 ± 9 years BP (Supplementary Methods and Table S2), and by clear annual $\delta^{18}O$ cycles and density bands (Supplementary Methods and Fig. S3).

Skeletal $\delta^{18}O$ was measured in fossil coral XM35 at approximately monthly resolution on a Finnigan MAT-251 mass spectrometer. For each sample aliquot, $200\pm20\,\mu g$ of powder was initially dissolved in 105% H_3PO_4 at 90 °C in an automated carbonate (Kiel) preparation device. The $\delta^{18}O$ values are reported relative to the Vienna PeeDee Belemnite (VPDB) using the NBS-19 ($\delta^{18}O=-2.20$‰) and NBS-18 ($\delta^{18}O=-23.0$‰) standards. The standard deviation for in-run $\delta^{18}O$ measurements on NBS-19 ($n=329$) was 0.04‰ during the course of the analysis. The average standard error for replicate $\delta^{18}O$ measurements for coral samples is 0.04‰($n=100$). The mean $\delta^{18}O$ value for XM35 (-4.77 ± 0.15‰1σ) is within the range of modern values for corals included in the stacked modern $\delta^{18}O$ record (Fig. 1 and Supplementary Fig. S4).

The age model for coral XM35 was established in the same way as for the modern coral microatoll record[24] (XM22), by assigning $\delta^{18}O$ maxima to early February. The $\delta^{18}O$ data were interpolated to give 12 values per year. The overall age model uncertainty for the coral time series is estimated as ±1 yr (see Supplementary Methods for further details). Shifting the monthly tie point by ±1 month has no effect on the results (Supplementary Discussion).

Comparisons of modern and fossil ENSO variability were made using: Kiritimati SST from ERSSTv3b (ref. 30) for 158° W, 2° N spanning March 1938 to May 2007; a compilation of Kiritimati Island modern coral $\delta^{18}O$ records[3,22,24] (modern coral $\delta^{18}O$ stack), spanning March 1938 to May 2007 (Supplementary Fig. S4 and Appendix); and the XM35 ~4.3 kyr BP coral $\delta^{18}O$ record (Supplementary Appendix). Comparisons of the annual cycle were made using a subset of the modern coral $\delta^{18}O$ stack (WM_stack modern coral $\delta^{18}O$ record; Supplementary Fig. S4 and Appendix) and Kiritimati SST from ERSSTv3b (ref. 30), for the period February 1978 to May 2007. These time series were broken down into trend, annual and residual (interannual) components, which occupy distinct spectral bins (Supplementary Fig. S5). Statistical analyses were performed on these components (Supplementary Methods).

Kiritimati SST data were obtained from the Extended Reconstructed Sea Surface Temperature version 3b data set[30], available from http://www.ncdc.noaa.gov/ersst/. Data for the modern coral $\delta^{18}O$ stack[3,22,24] are available from http://hurricane.ncdc.noaa.gov/pls/paleox/f?p=519:1:459649581239080::::P1_STUDY_ID:1847 and http://hurricane.ncdc.noaa.gov/pls/paleox/f?p=519:1:0::::P1_STUDY_ID:12278.

Data from the ~4.3 kyr BP coral (XM35) are tabulated in the Supplementary Appendix and are archived at WDC Paleoclimatology: ftp://ftp.ncdc.noaa.gov/pub/data/paleo/coral/east_pacific/kiritimati2013.txt and ftp://ftp.ncdc.noaa.gov/pub/data/paleo/coral/east_pacific/kiritimati2013.xls

Received 8 June 2013; accepted 2 August 2013; published online 5 September 2013; corrected online 6 September 2013

References

1. Tudhope, A. W. *et al.* Variability in the El Niño-Southern Oscillation through a glacial–interglacial cycle. *Science* **291,** 1511–1517 (2001).
2. Moy, C. M., Seltzer, G. O., Rodbell, D. T. & Anderson, D. M. Variability of El Niño/Southern Oscillation activity at millennial timescales during the Holocene epoch. *Nature* **420,** 162–165 (2002).
3. Woodroffe, C. D., Beech, M. R. & Gagan, M. K. Mid-late Holocene El Niño variability in the equatorial Pacific from coral microatolls. *Geophys. Res. Lett.* **30,** 1358 (2003).
4. McGregor, H. V. & Gagan, M. K. Western Pacific coral $\delta^{18}O$ records of anomalous Holocene variability in the El Niño-Southern Oscillation. *Geophys. Res. Lett.* **31,** L11204 (2004).
5. Conroy, J. L., Overpeck, J. T., Cole, J. E., Shanahan, T. M. & Steinitz-Kannan, M. Holocene changes in eastern tropical Pacific climate inferred from a Galápagos lake sediment record. *Quat. Sci. Rev.* **27,** 1166–1180 (2008).
6. Koutavas, A. & Joanides, S. El Niño-Southern Oscillation extrema in the Holocene and Last Glacial Maximum. *Paleoceanography* **27,** PA4208 (2012).
7. Clement, A. C., Seager, R. & Cane, M. A. Suppression of El Niño during the mid-Holocene by changes in the Earth's orbit. *Paleoceanography* **15,** 731–737 (2000).
8. Liu, Z., Kutzbach, J. & Wu, L. Modeling climate shift of El Nino variability in the Holocene. *Geophys. Res. Lett.* **27,** 2265–2268 (2000).
9. Zheng, W., Braconnot, P., Guilyardi, E., Merkel, U. & Yu, Y. ENSO at 6ka and 21ka from ocean–atmosphere coupled model simulations. *Clim. Dyn.* **30,** 745–762 (2008).
10. Brown, J. R., Tudhope, A. W., Collins, M. & McGregor, H. V. Mid-Holocene ENSO: Issues in quantitative model-proxy data comparisons. *Paleoceanography* **23,** PA3202 (2008).
11. Cobb, K. M. *et al.* Highly variable El Niño–Southern Oscillation throughout the Holocene. *Science* **339,** 67–70 (2013).
12. Ropelewski, C. F. & Halpert, M. S. Global and regional scale precipitation patterns associated with the El Niño/Southern Oscillation. *Mon. Weath. Rev.* **115,** 1606–1626 (1987).
13. Cane, M. A. The evolution of El Niño, past and future. *Earth Planet. Sci. Lett.* **230,** 227–240 (2005).
14. Guilyardi, E. *et al.* Understanding El Niño in ocean–atmosphere general circulation models: Progress and challenges. *Bull. Am. Meteorol. Soc.* **90,** 325–340 (2009).
15. Collins, M. *et al.* The impact of global warming on the tropical Pacific Ocean and El Niño. *Nature Geosci.* **3,** 391–397 (2010).
16. Yeh, S-W. *et al.* El Niño in a changing climate. *Nature* **461,** 511–514 (2009).
17. Cole, J. E., Fairbanks, R. G. & Shen, G. T. Recent variability in the Southern Oscillation: Isotopic results from a Tarawa Atoll coral. *Science* **260,** 1790–1793 (1993).
18. Cobb, K. M., Charles, C. D., Cheng, H. & Edwards, R. L. El Niño/Southern Oscillation and tropical Pacific climate during the last millennium. *Nature* **424,** 271–276 (2003).
19. Li, J. *et al.* Interdecadal modulation of El Niño amplitude during the past millennium. *Nature Clim. Change* **1,** 114–118 (2011).
20. Braconnot, P., Luan, Y., Brewer, S. & Zheng, W. Impact of Earth's orbit and freshwater fluxes on Holocene climate mean seasonal cycle and ENSO characteristics. *Clim. Dyn.* **38,** 1081–1092 (2012).
21. Wittenberg, A. T. Are historical records sufficient to constrain ENSO simulations? *Geophys. Res. Lett.* **36,** L12702 (2009).
22. Evans, M. N., Fairbanks, R. G. & Rubenstone, J. L. A proxy index of ENSO teleconnections. *Nature* **394,** 732–733 (1998).
23. Torrence, C. & Webster, P. J. The annual cycle of persistence in the El Niño/Southern Oscillation. *Quart. J. R. Meteorol. Soc.* **124,** 1985–2004 (1998).
24. McGregor, H. V., Fischer, M., Gagan, M. K., Fink, D. & Woodroffe, C. D. Environmental control of the oxygen isotope composition of Porites coral microatolls. *Geochim. Cosmochim. Acta* **75,** 3930–3944 (2011).
25. Li, T. & Philander, S. G. H. On the annual cycle of the eastern equatorial Pacific. *J. Clim.* **9,** 2986–2998 (1996).
26. Haug, G. H., Hughen, K. A., Sigman, D. M., Peterson, L. C. & Röhl, U. Southward migration of the Intertropical Convergence Zone through the Holocene. *Science* **293,** 1304–1308 (2001).
27. Carré, M. *et al.* Mid-Holocene mean climate in the south eastern Pacific and its influence on South America. *Quat. Int.* **253,** 55–66 (2012).
28. Timmermann, A., Lorenz, S. J., An, S-I., Clement, A. & Xie, S-P. The effect of orbital forcing on the mean climate and variability of the tropical Pacific. *J. Clim.* **20,** 4147–4159 (2007).
29. Fowler, A. M. *et al.* Multi-centennial tree-ring record of ENSO-related activity in New Zealand. *Nature Clim. Change* **2,** 172–176 (2012).
30. Smith, T. M., Reynolds, R. W., Peterson, T. C. & Lawrimore, J. Improvements to NOAA's historical merged land-ocean surface temperature analysis (1880-2006). *J. Clim.* **21,** 2283–2296 (2008).

Acknowledgements

We thank J. Bryden, T. Schambron and A. T. Berenti for support with fieldwork carried out under Permit from the Environment and Conservation Division, Ministry of Environment, Lands and Agriculture Development of the Republic of Kiribati. D. Zeko, J. Gaudry, A. Harbeck and S. Maher assisted with sample preparation. J. Abrantes is thanked for XRD analyses and thin-section preparation. J. Cowley, H. Scott-Gagan, J. Cali, A. McGregor, W. Lees and S. Sosdian assisted with oxygen isotope analysis. M. Dore, L. Glasbergen and H. Schofield assisted with Sr/Ca analysis. A. Wittenberg, J. Smerdon and R. Seager assisted with GFDL CM2.1 model output. M. Evans, N. J. Abram and T. J. Williams are thanked for thoughtful comments on the manuscript. We acknowledge the support of J-x. Zhao and funding from Australian Research Council (ARC) LIEF grant LE0989067 for MC-ICPMS U–Th dating. This work was supported by ARC Discovery Projects grants DP0664313 (C.D.W.), DP1092945 (H.V.M.) and DP063227 (M.K.G.), AINSE Awards AINGRA10077 (H.V.M.) and AINGRA09021 (H.V.M.), ANSTO 'Cosmogenic climate Archives of the Southern Hemisphere' and 'Isotopes in Climate Change and Atmospheric Systems' projects, and the National Computational Merit Allocation Scheme (S.J.P.). H.V.M. is supported by an AINSE Fellowship.

Author contributions

H.V.M, C.D.W. and D.F. conducted fieldwork, sampled fossil coral XM35 and designed the study. H.V.M. oversaw all analytical aspects of the study, with contributions to $\delta^{18}O$ analysis from M.K.G., age dating from C.D.W. and D.F., and Sr/Ca analysis from H.W. S.J.P. provided climate model output and analysis and assisted with the coral age model. M.J.F. and H.V.M. conducted the statistical analysis. H.V.M. and M.K.G. wrote the manuscript with assistance from M.J.F. All authors discussed the results, interpretations and contributed to the final version of manuscript.

Additional information

Supplementary information is available in the online version of the paper. Reprints and permissions information is available online at www.nature.com/reprints. Correspondence and requests for materials should be addressed to H.V.M.

Competing financial interests

The authors declare no competing financial interests.

ERRATUM

A weak El Niño/Southern Oscillation with delayed seasonal growth around 4,300 years ago

H. V. McGregor, M. J. Fischer, M. K. Gagan, D. Fink, S. J. Phipps, H. Wong and C. D. Woodroffe

Nature Geosci. http://dx.doi.org/10.1038/ngeo1936; published online 5 September 2013; corrected online 6 September 2013

In the version of this Letter originally published online, the published online date should have read '5 September 2013'. This has been corrected in the PDF and HTML versions of the Letter.